We are IntechOpen, the world's leading publisher of Open Access books
Built by scientists, for scientists

6,900
Open access books available

186,000
International authors and editors

200M
Downloads

154
Countries delivered to

Our authors are among the

TOP 1%
most cited scientists

12.2%
Contributors from top 500 universities

CLARIVATE ANALYTICS
BOOK CITATION INDEX
INDEXED

WEB OF SCIENCE™

Selection of our books indexed in the Book Citation Index
in Web of Science™ Core Collection (BKCI)

Interested in publishing with us?
Contact book.department@intechopen.com

Numbers displayed above are based on latest data collected.
For more information visit www.intechopen.com

Insights into the Mechanism of Photocatalytic Degradation of Volatile Organic Compounds on TiO$_2$ by Using In-situ DRIFTS

Song Sun and Fan Zhang

Additional information is available at the end of the chapter

Abstract

Photocatalytic degradation is a cost-effective technology for the removal of volatile organic compounds. However, the mechanism of photocatalytic degradation of volatile organic compounds on TiO$_2$ is still a challenging issue. Fortunately, infrared spectroscopy is a powerful technique, able to provide information about adsorption/desorption, intermediates/products, and interfacial reaction. The aim of this chapter is to review several aspects of our current understanding of the role of TiO$_2$ in the degradation of volatile organic compounds, by using in situ diffuse reflectance infrared Fourier transform spectroscopy. We firstly review the state of photocatalytic degradation of volatile organic compounds briefly. This is followed by a summary of in situ infrared techniques. The interaction of TiO$_2$ surfaces with vapor organic molecules and other species is then reviewed with the representative works in recent years. It ends with a brief future outlook on the mechanism of photocatalytic air purification of TiO$_2$.

Keywords: infrared spectroscopy, photocatalysis, volatile organic compounds, TiO$_2$, DRIFTS, air purification

1. Introduction

Volatile organic compounds (VOCs), such as toluene, formaldehyde, and benzene, emitted from decoration materials, paint and cementing compound, are the major pollutants in indoor air [1]. There is evidence that most of the VOCs significantly impact human health. In general, they can irritate the mucous membranes of eyes and respiratory tract, and even damage the nervous system [2,3]. Compared with adsorption by activated carbon, biofiltration, or thermal cataly-

sis, photocatalytic degradation is a cost-effective technology for removal of VOCs, because the pollutants can be oxidized to mineral salts, CO_2, and H_2O under mild operating conditions [4,5]. In a typical process, a semiconductor is irradiated with light whose energy is higher than the band gap energy of the semiconductor, generating an electron (e^-) from the valence band to the conduction band and leaving a hole (h^+) in the valence band. Some electron–hole charge carriers can in turn undergo recombination and dissipate the excess energy, while the other carriers can migrate to the surface of the semiconductor and initiate redox reactions with the surface-adsorbed organic compounds.

One of the most widely used semiconductor photocatalysts at present is TiO_2, due to its good chemical and thermal stabilities, low cost, innocuousness, and relatively high photocatalytic activity [7–9]. As evidenced by a wide number of publications that have appeared in the past 20 years, the photocatalytic degradation of VOCs on TiO_2 mainly involves three aspects:

i. Given that TiO_2 possesses the relatively large band gap (3.2 eV) so that only UV radiation can activate it, many modification methods, including ion doping and semiconductors coupling, are developed on TiO_2 to use low-energy photons available in the visible spectral region. In the meantime, efforts have been made to enhance its photocatalytic performance by increasing the electron–hole pair separation and/or specific surface area.

ii. Photocatalytic reactor development, as an engineering approach to enhance the efficiency of degradation of VOCs, involves updating existing fixed and flow bed reactors, and designing new reactors.

iii. Various researchers were dedicated to interpreting the mechanism and kinetics of photocatalytic degradation of VOCs. Since the photocatalytic degradation of VOCs is a complicated process and critically depends on the temperature, humidity level, pressure, and the composition of the reaction's gaseous environment, it is desirable to identify the mechanism to help researchers rational design new photocatalysts and reactors for better photocatalytic activities of degradation of VOCs.

Until now, the use of infrared (IR) spectroscopy has become one of the most powerful techniques to study the photocatalytic mechanism of degradation of VOCs with the advent of in situ accessories [10,11]. A greater variety of important information about the nature of adsorbed molecules and reaction intermediates can be obtained by using IR. In many cases, it has been possible to establish relationships between surface properties of photocatalysts, interactions of interfacial species, and the changes of these species and the photocatalytic activities. The improved understanding obtained from such in situ IR characterizations has led to the developments of new photocatalysts and better understanding of photocatalytic processes. We have also noticed that some reviews and books had highlighted the representative examples in this field [12,13]. Given that the mechanism of photocatalytic degradation of VOCs on TiO_2 is still a challenging issue, herein, we review several aspects of our current understanding of the role of TiO_2 in the degradation of VOCs by using in situ diffuse reflectance infrared Fourier transform spectroscopy (DRIFTS). Special interest is taken in describing the interaction of TiO_2 surfaces with vapor organic molecules and other species, considering that

the target pollutants, humidity level and oxygen play an important role in TiO$_2$ photocatalysis in gaseous. A summary of the remaining challenges and prospects of in situ IR for photocatalytic air purification investigation is also given.

2. In situ DRIFTS technique and related accessories

IR is the vibrational technique based on the interaction of electromagnetic radiation with species that possess a permanent or induced dipole moment and the excitation of different vibrational states [14]. The test forms of IR mainly include transmission/absorption spectroscopy, internal reflection spectroscopy (IRS) which is well known for attenuated total reflection (ATR), and DRIFTS. In principle, DRIFTS is most suitable for in situ measurements of gas–solid interface reaction, especially for photocatalytic degradation of VOCs on solid photocatalysts, because it can collect and analyze the surface-reflected electromagnetic radiation carrying surface and interfacial information. As shown in **Figure 1**, the regular and specular reflection from the photocatalyst powders with infrared beam incidence can be obtained by using a particular reflection light collector. Moreover, this collection mode allows the introduction of gaseous species to the surface of the photocatalysts so that the in situ experimental condition can be achieved [10,15].
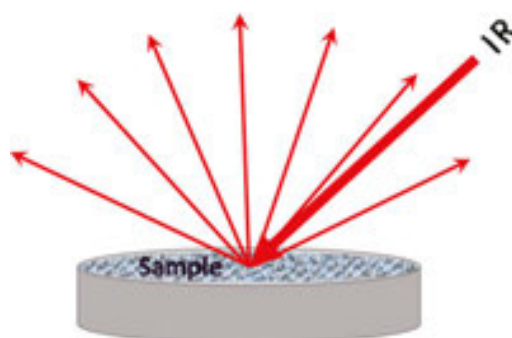

Figure 1. Basic scheme of DRIFTS technique.

Generally, an in situ DRIFTS experimental apparatus consists of one reaction cell, one diffuse reflectance accessory, and one gas-dosing system. A typical design of the diffuse reflectance accessory with on-axis geometry (**Figure 2**) has a higher optical efficiency than the other designs, off-axis accessory and integrating spheres [16]. However, one major drawback of on-axis geometry is that much of the front-surface reflection is collected along with the diffusely reflected reflection that has penetrated into the sample before reemerging from its top surface. It means that bands become distorted, and the ratio of the absorption coefficient and the scattering coefficient versus concentration becomes nonlinear at low concentration [16]. All specularly reflected radiation can be eliminated by accessories with off-axis design (**Figure 3a**). In this case, it should be pointed out that band shapes are more symmetrical, apart from the contribution of compensation by the Kubelka–Munk transform,

$$f(R) = (1 − R)^2/2R = 2.3ac/s,$$

where R is absolute reflectivity, a is absorbance, c is concentration, and s is scattering coefficient.
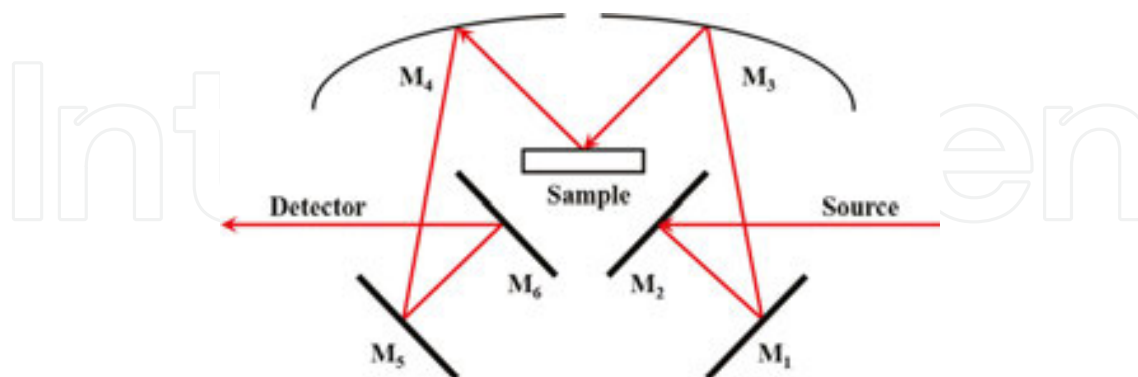
Figure 2. The principle of DRIFTS accessory with on-axis optical geometry. M_1, M_2, M_5, and M_6 are plane mirrors, while M_3 and M_4 are opposed ellipsoids (©2007 John Wiley & Sony Inc. [16]).

Commercial DRIFTS accessories usually consist of the reaction cell covered by a dome with three windows (**Figure 3b,c**) for solid–gas interfacial investigation in photocatalysis. Two of them are IR-transparent windows for the spectrometer infrared beam to enter and exit the cell, while the third one allows for observation or irradiation by excitation light source on photo-catalysts. IR-transparent windows can be made of KBr, ZnSe, and CaF_2 for mid-infrared test, and polyethylene (PE), Ge, and Si for far-infrared test, respectively. Quartz is the common material for viewing window.
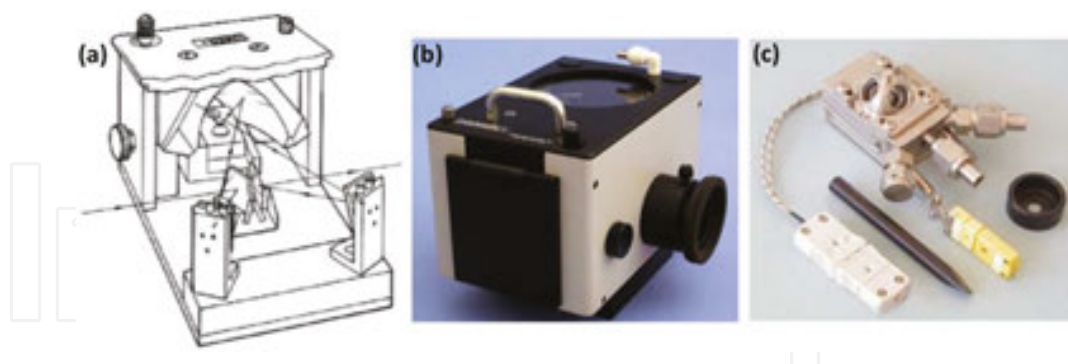

Figure 3. (a) Interior view of Harrick Scientific's Praying Mantis DRIFTS accessory with off-axis design, and images of (b) Harrick Scientific's DRIFTS accessory product, and (c) reaction cell enclosed with a dome with three windows. The cell enables a reaction gas to be introduced and reacted with the sample so that the reaction can be studied in situ.

In situ experimental conditions can be achieved by coupling the gas-dosing system with DRIFTS accessory and its cell. Photocatalytic air purification, compared with degradation in aqueous, water splitting and CO_2 reduction, seldom uses commercial gas-dosing systems to meet the requirement of DRIFTS investigation, because the gas-dosing system should offer each reaction gas with different concentrations, flow rates and humidity levels in a wide range,

and different residual gas absorbers for different VOCs. Therefore, the gas-dosing system was always built by independent groups. **Figure 4** shows the schematic diagram of the gas-dosing system for photocatalytic air purification and in situ DRIFTS measurements by Zhang et al. [17,18]. Take toluene for example; mass flow controllers were used to control the 20 vol% O$_2$/N$_2$ compressed air which carried toluene vapor from the saturator containing toluene. The water vapor was supplied to the cell via a bypass line. Argon (Ar) was used as purging gas. In the experiment, the accurate concentration of toluene was analyzed by gas chromatography. The relative humidity (RH%) in the cell was determined using an electronic hygrometer fixed in the bypass line. The whole system operating interface has been renovated based on the previous study for convenience and user-friendliness (**Figure 5**).
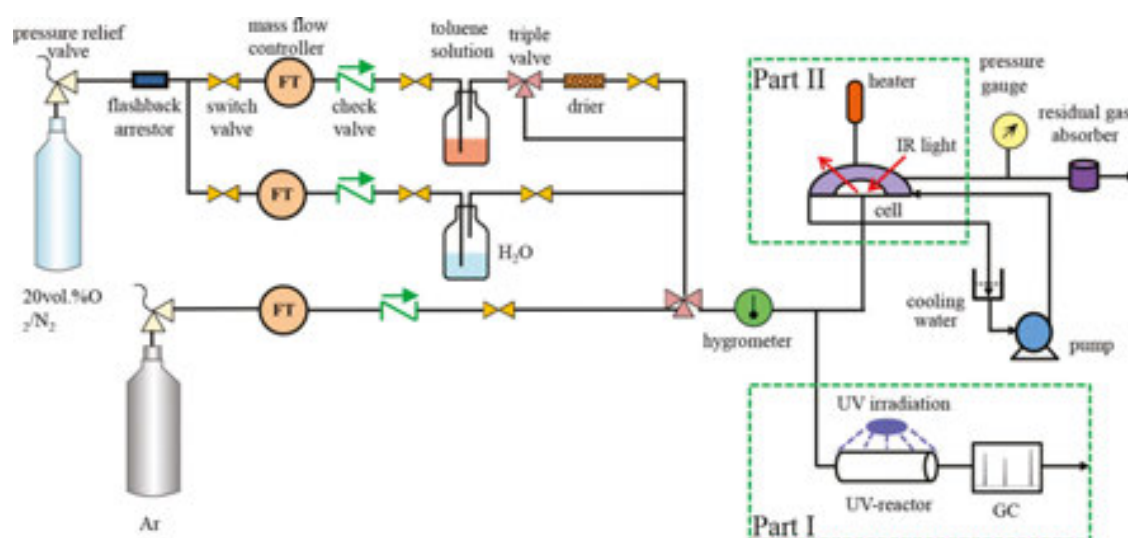
Figure 4. Schematic diagram of the gas-dosing system for (Part I) the photocatalytic activity and (Part II) in situ DRIFTS (©2015 Elsevier [17]).
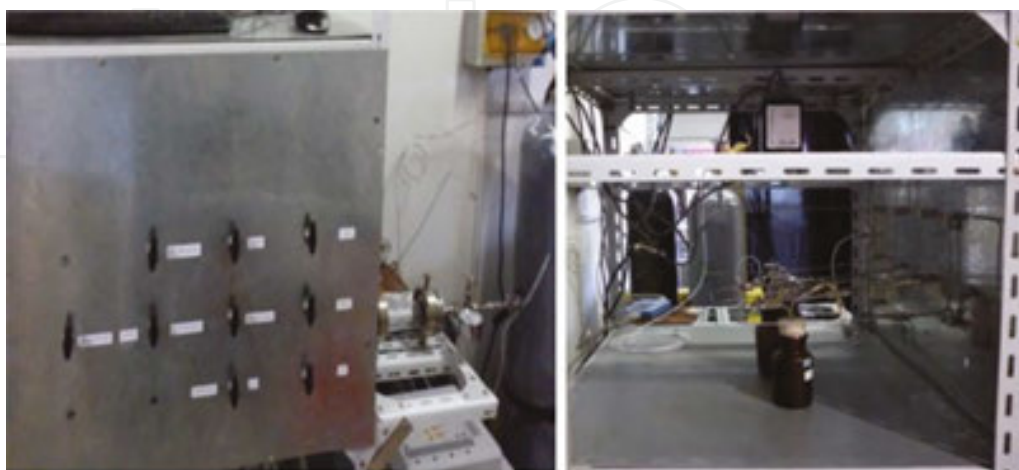
Figure 5. Images of the operating interface of reaction gas-dosing system for in situ DRIFTS test (©2014 Springer [18]).

The setup reported by Deveau et al. [23–25]. But describing in situ IR cells and gas-dosing system in DRIFTS investigation in photocatalysis is the scope of the present view. It can be concluded that although DRIFTS provides a useful means for gathering information concerning the photocatalytic air purification, it is still on the initial stage, both for in situ cells and gas-dosing systems.

## 3. In situ DRIFTS investigation of photocatalytic degradation of VOCs on TiO$_2$

Although many studies have focused on photocatalytic degradation of VOCs on TiO$_2$, the reaction mechanism and a comprehensive picture of the adsorption structure and degradation route are unclear or remain controversial. In principle, the photogenerated e$^-$ and h$^+$ can directly initiate redox reaction with surface-adsorbed molecules of VOCs: electron donors (D$_{ads}$) and acceptor (A$_{ads}$) on TiO$_2$, respectively. If multiple kinds of electron donors (D$_{ads}$) and/or acceptor (A$_{ads}$) are present on the surface, however, the e$^-$ and h$^+$ may be trapped to form secondary radicals which further react with the target VOCs. For pure TiO$_2$, its surface coordinatively unsaturated Ti^{4+} and O^{2-} species allow dissociative chemisorption of molecular water to satisfy the coordination of Ti^{4+} and O^{2-} sites, making the surface of TiO$_2$ hydroxylated [31–33], making the air purification complex. Here, some representative works in recent years and several examples from our group are discussed.

3.1. Degradation of toluene

Reports have shown that surface hydroxyl groups formed by water vapor interacting with TiO$_2$ surface can easily affect the adsorption and photocatalytic processes of toluene degradation. Augugliaro and coworkers [34] carried out the toluene and toluene/water adsorption experiments on TiO$_2$ samples. The corresponding IR spectra are shown in **Figure 6**. Curve a is the spectrum of the TiO$_2$ powder pre-outgassed at room temperature, exhibiting a peak at 3665 cm^{-1} and a very broad adsorption in the high wavenumber region. These components can be assigned to the stretching mode of free hydroxyl groups, hydrogen-bonded OH groups, and water molecules coordinated to surface Ti^{4+}. In contact with toluene, the band at 3665 cm^{-1}, due to the free hydroxyl groups, completely disappeared, indicating that free hydroxyl groups are effective Lewis acid adsorption sites for toluene, and a new broad and complex band appeared at lower wavenumber region, the shift resulting from the interaction between the OH groups and the π electrons of the aromatic molecules. In addition, peaks due to adsorbed toluene appeared in the 3100–2800 cm^{-1} (CH stretching) and 1610–1360 cm^{-1} (ring stretching, CH deformation) ranges. After short outgassing at room temperature, the bands of the adsorbed toluene disappeared, and the characteristic bands of the free OH species were completely restored (curve c), indicating that the interaction between aromatic molecules and hydroxyl group is quite weak and fully reversible.
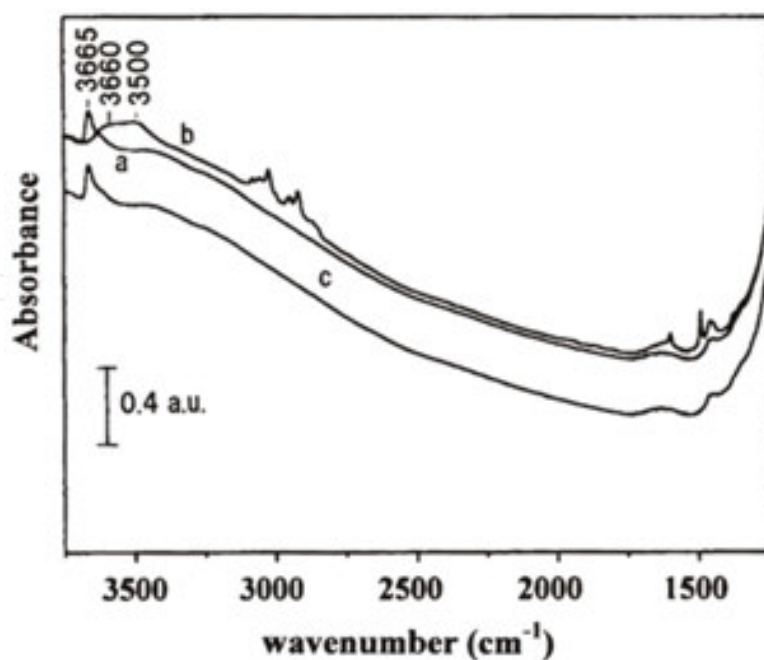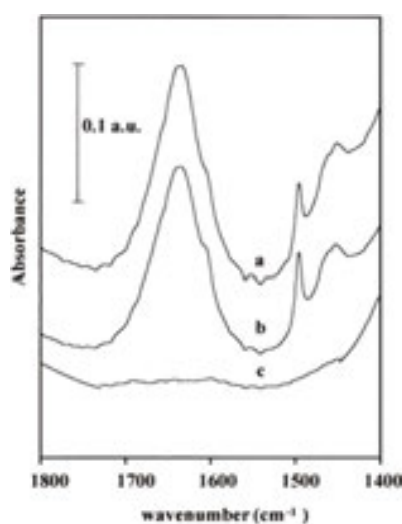
Figure 6. IR spectra of TiO$_2$: (a) outgassed at room temperature for 45 min; (b) in contact with 3 Torr toluene; (c) after 5 min re-outgassing at room temperature (©2015 Elsevier [34]).
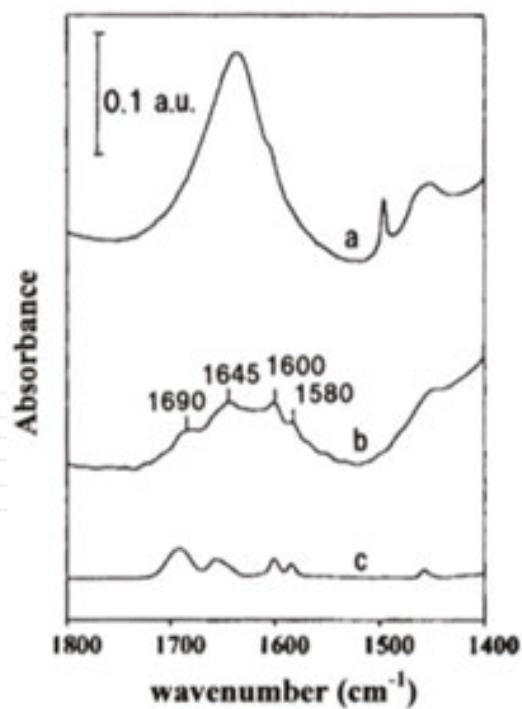
Figure 7. IR results for the photo-oxidation of toluene on the TiO$_2$ pre-outgassed at room temperature. IR spectra of TiO$_2$: (a) in the presence of the toluene/H$_2$O/O$_2$ mixture, (b) after 10 min UV irradiation and subsequent outgassing at room temperature for 45 min, (c) in the presence of benzaldehyde (©2015 Elsevier [34]).

Then they investigated toluene photocatalytic oxidation on two TiO_2 samples with different surface hydration states: one pre-outgassed at room temperature and the other pre-outgassed at 873 K without the occurrence of the anatase–rutile phase transition. **Figure 7** shows the results of the toluene photocatalytic oxidation experiment obtained in the case of TiO_2 pre-outgassed at room temperature. After exposing TiO_2 to the toluene/H_2O/O_2 mixture, bands due to adsorbed water (peak at 1640 cm^{-1}) and aromatic molecules (signals at 1600, 1496, and 1460 cm^{-1}) were observed (**Figure 7a**). After irradiation, a slight decrease in the toluene bands at 1496 and 1460 cm^{-1} was observed, while new bands appeared (**Figure 7b**). This suggested that a fraction of toluene transformed to a new species under UV irradiation. Finally, they found that the main oxidation product of toluene was benzaldehyde. In the case of the dehydroxylated TiO_2, the admission of the toluene/H_2O/O_2 mixture onto the TiO_2 produced bands due to physically adsorbed water and toluene molecules (**Figure 8a**). Nevertheless, after UV irradiation, traces of bands due to benzaldehyde were hardly recognizable in the spectrum (**Figure 8c**). Compared with the fully hydroxylated TiO_2, the dehydroxylated one exhibited strongly reduced photocatalytic activity, confirming that surface OH groups play an important role in the photocatalytic oxidative process.


Figure 8. IR results for the photo-oxidation of toluene on the TiO_2 pre-outgassed at 873 K. IR spectra of TiO_2: (a) in the presence of the toluene/H_2O/O_2 mixture, (b) after exposure to the UV light for 10 min, (c) after subsequent outgassing at room temperature for 45 min (©2015 Elsevier [34]).

Maira et al. [35] studied the photocatalytic activities of TiO_2 which are prepared by thermal and hydrothermal methods, respectively, for the gas-phase photocatalytic oxidation of toluene. A comparative IR study of the surface structure of the samples was also conducted. **Figure 9** shows the results of photocatalytic oxidation of toluene on the TiO_2 prepared by thermal method. Upon adsorption of toluene, the bands (3630, 3674, and 3687 cm^{-1}) of the isolated hydroxyl groups were replaced by a broad band centered at 3550 cm^{-1} (**Figure 9c**), indicating that toluene was mainly adsorbed on the isolated hydroxyl groups at the TiO_2 prepared by thermal method. The irradiation of TiO_2 under H_2O/O_2 condition (**Figure 9d**) caused a slight decrease of the bands due to the adsorbed toluene (3085, 3066, 3027, 3927, and

2872 cm^{-1}) and the formation of several small bands due to benzaldehyde in the 1900–1100 cm^{-1} range. The band at 1682 cm^{-1} was attributed to the carbonyl vibration of the aldehyde group, and the bands at 1641, 1595, and 1580 cm^{-1} may arise from the different vibrational modes of the aromatic ring. After a subsequent outgassing at room temperature (**Figure 9e**), the 3550 cm^{-1} band and the bands due to adsorbed toluene practically disappeared, and the bands of isolated hydroxyls were partially recovered. This indicated that toluene was weakly adsorbed on the hydroxyls. In addition, the decrease of the bands due to benzaldehyde indicated that a small amount of benzaldehyde was also desorbed. After exposing the treated sample to water vapor and subsequent irradiation, the bands due to benzaldehyde reduced but did not disappear. Toluene adsorption on the TiO$_2$ prepared by hydrothermal method resulted in several changes. Toluene was adsorbed not only on the isolated hydroxyls, but also on the H-bonded hydroxyls. The irradiation of TiO$_2$ under H$_2$O/O$_2$ condition caused decrease of toluene and hydroxyl species, and formation of benzaldehyde. A subsequent outgassing of the sample resulted in the disappearance of the bands related to toluene adsorption and a slight decrease of the adsorbed benzaldehyde bands. By considering the photocatalytic activity of these two samples and the IR results, they concluded that the interaction of toluene with the hydroxyl groups of isolated types mainly leads to the formation of benzaldehyde, while the interaction with H-bonded hydroxyls leads to nearly complete degradation. Both types of hydroxyl groups are lost during the reaction, which produces a decrease in the photocatalytic degradation of toluene. The photocatalytic degradation of toluene adsorbed on H-bonded hydroxyls can be regenerated in the presence of water vapor.
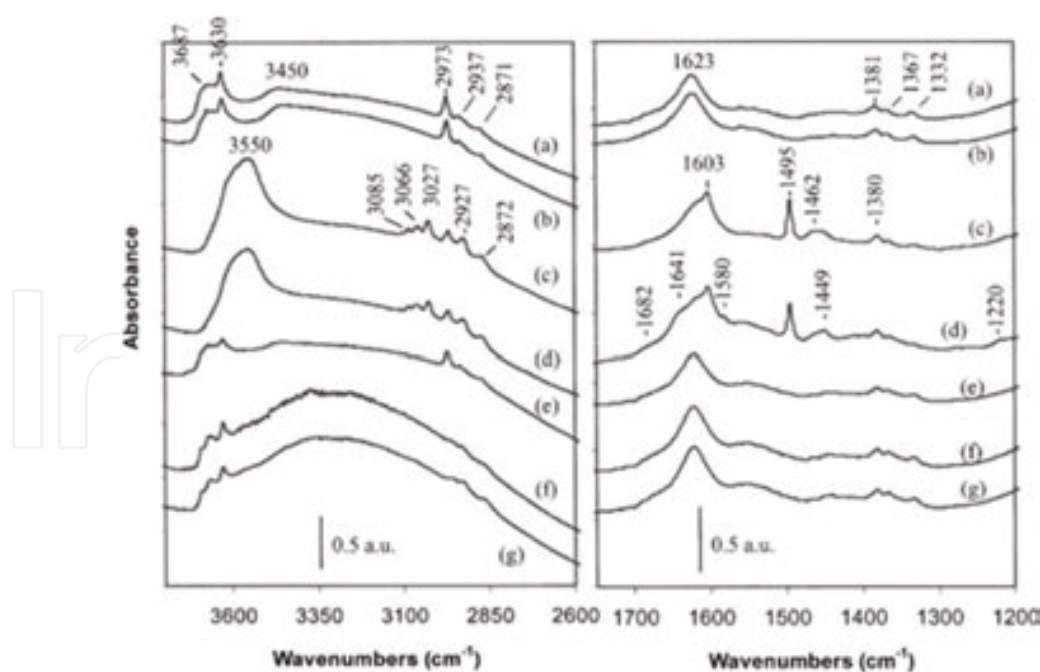

Figure 9. IR spectra of TiO$_2$ prepared by thermal method after the following treatments performed at room temperature: (a) evacuation for 15 min, (b) evacuation for 2 h, (c) introduction of 5 Torr of toluene into IR cell and subsequent introduction of 50 Torr of oxygen, (d) irradiation for 30 min, (e) evacuation of the sample for 15 min, (f) introduction of 5 Torr of H$_2$O into the cell, and (g) irradiation for 30 min (©2001 Elsevier [35]).
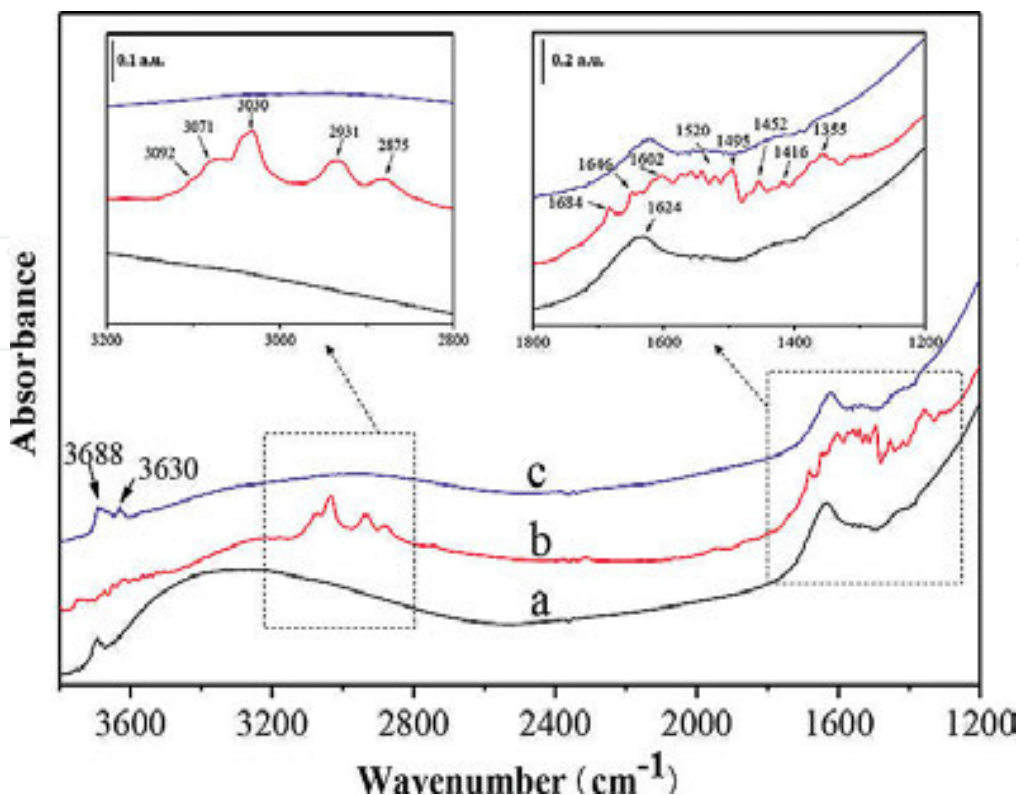
Figure 10. In situ DRIFTS spectra of (a) fresh Fe–TiO$_2$, (b) Fe–TiO$_2$ used for 20 consecutive reaction runs, and (c) Fe–TiO$_2$ after heat-treatment at 653 K for 3 h (©2012 Elsevier [40]).

Ibusuki et al. [37–39]. Our group has also carried out some research on the photocatalytic degradation of toluene by using in situ DRIFTS. Sun et al. [40] found that the Fe–TiO$_2$ photocatalyst was partially deactivated after 20 consecutive reaction runs. A DRIFTS experiment was then performed to investigate the deactivation mechanism, and the results are shown in **Figure 10**. From **Figure 10a**, the surface of a fresh photocatalyst was relatively clean. After 20 consecutive reaction runs, many new bands appeared (**Figure 10b**). The bands at 3092, 3071, 3030, 2931, 2875, 1646, 1602, 1495, 1452, and 1355 cm^{-1} were due to the adsorbed toluene on the surface of the photocatalyst. The band at 1684 cm^{-1} was attributed to the carbonyl vibration of the aldehyde group, and the bands at 1520 and 1416 cm^{-1} may arise from the asymmetric and symmetric vibrations of the COO$^-$ group. This result indicated that the intermediates benzaldehyde and benzoic acid were formed during the photocatalytic degradation of toluene. After heat treatment at 653 K for 3 h in air, the bands of benzaldehyde and benzoic acid disappeared completely (**Figure 10c**). From this experiment, the reason for deactivation was attributed to the formation of stable intermediates, such as benzaldehyde and benzoic acid, which occupied the active sites on the surface of the photocatalyst. These intermediates can be removed with heat treatment at 653 K for 3 h, and the deactivated photocatalyst can be regenerated completely.
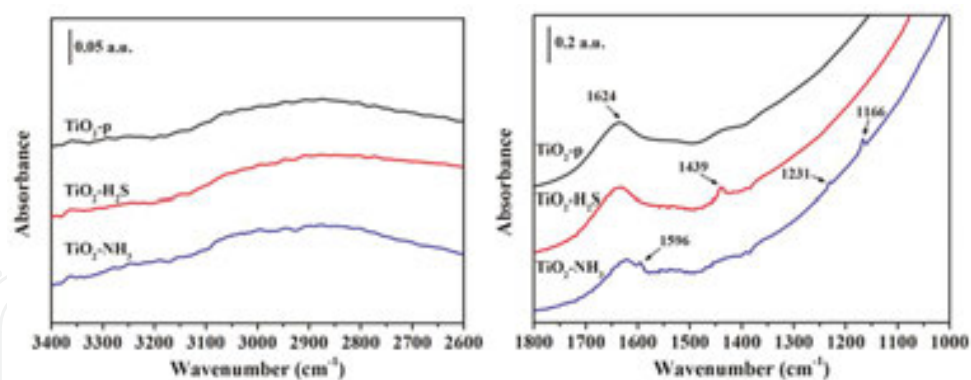
Figure 11. DRIFTS spectra of TiO$_2$–p, TiO$_2$ modified with H$_2$S, and TiO$_2$ modified with NH$_3$ (©2015 Elsevier [17]).
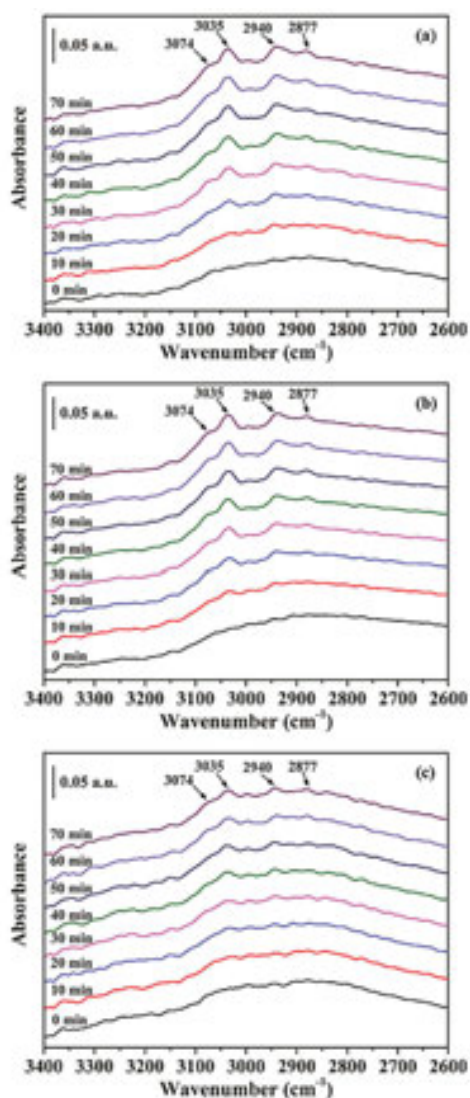
Figure 12. In situ DRIFTS spectra of toluene adsorption on (a) TiO$_2$–p, (b) TiO$_2$–H$_2$S, and (c) TiO$_2$–NH$_3$ photocatalysts (©2015 Elsevier [17]).

In order to understand the influences of H_2S/NH_3 species on the photocatalytic degradation of toluene on TiO_2, Zhang et al. [17] investigated the adsorption and photocatalytic degradation of gaseous toluene on TiO_2 surface modified with H_2S and NH_3 species. **Figure 11** shows the DRIFTS spectra of the samples. The surface of fresh TiO_2 (TiO_2-p) was relatively clean. A small band attributed to the bending vibration of δ(H–S) was observed at 1439 cm^{-1} (curve TiO_2–H_2S), suggesting the presence of sulfhydryl on the TiO_2–H_2S surface. In the curve TiO_2–NH_3, the band at 1596 cm^{-1} was attributed to the coordinated NH_3, and the bands at 1231 and 1166 cm^{-1} were due to the symmetric deformation of NH_3. **Figure 12** shows the DRIFTS spectra of toluene adsorbed on the samples. After toluene was introduced, the characteristic bands of toluene (3074, 3035, 2940, and 2877 cm^{-1}) appeared. The intensities of these bands on TiO_2–NH_3 were obviously weaker than those on TiO_2–H_2S and TiO_2–p after 70 min of adsorption, indicating that the adsorption capacity of TiO_2–NH_3 for toluene is smaller than those of TiO_2–p and TiO_2–H_2S. After the adsorption of toluene reached equilibrium, the samples were irradiated by UV light (**Figure 13**). In the high wavenumber region, the characteristic bands of toluene decreased in different degrees for all the samples, indicating that adsorbed toluene was decomposed. In the low wavenumber region, many bands of benzaldehyde and benzoic acid appeared, and these bands on TiO_2–H_2S were significantly strengthened, suggesting that there were more intermediates on TiO_2–H_2S. Combined with the results of photocatalytic activity and other characterizations of the samples, it is concluded that surface modification with H_2S enhanced the adsorption of toluene and promoted the degradation rate at the start of photocatalytic degradation, while that with NH_3 inhibited the adsorption of toluene but enhanced the photocatalytic activity for the degradation of toluene. For TiO_2–H_2S, the sulfhydryl group formed from the dissociation of H_2S molecules was favorable for toluene adsorption. The low photocatalytic activity may be caused by the inhibition of the regeneration of surface hydroxyl groups, poor generation of $O^{2-}\bullet$ radicals, and accumulation of highly stable intermediates. For TiO_2–NH_3, steric hindrance interfered with the adsorption of toluene, while the abundant surface hydroxyl groups were likely to contribute to the degradation of toluene.
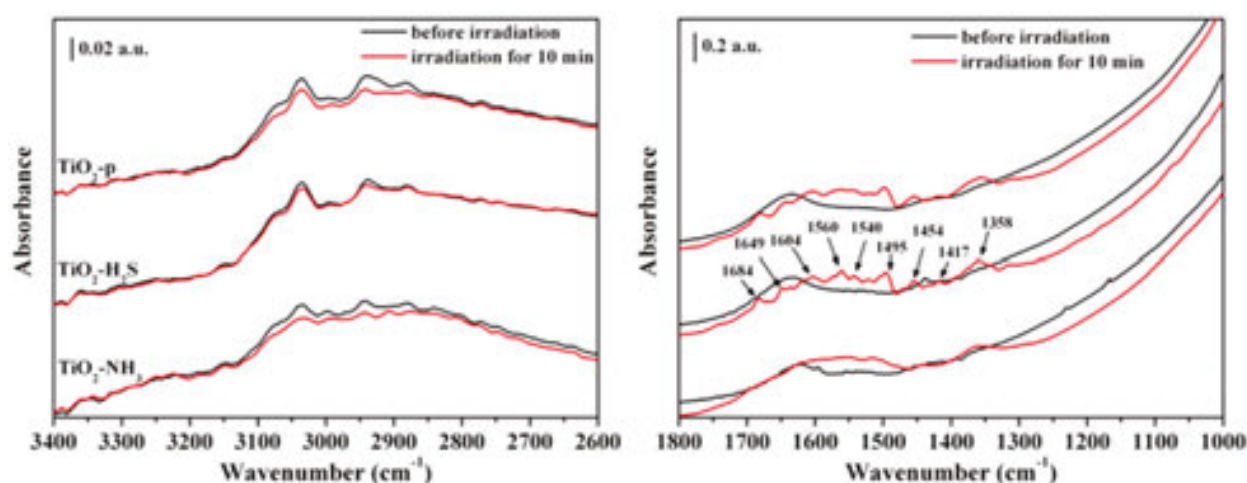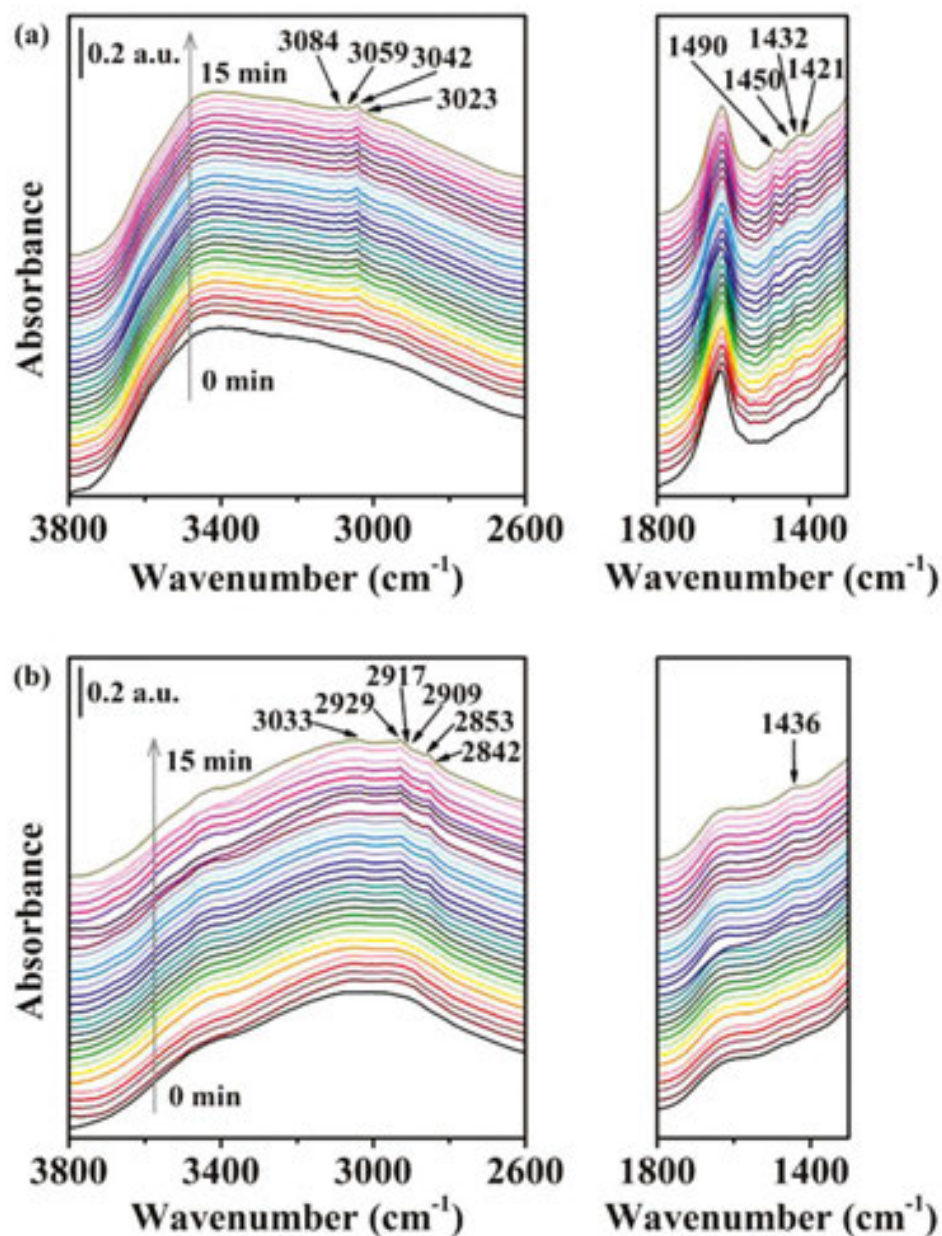

Figure 13. In situ DRIFTS spectra of toluene oxidation on (a) TiO_2–p, (b) TiO_2–H_2S, and (c) TiO_2–NH_3 photocatalysts with UV irradiation (©2012 Elsevier [17]).
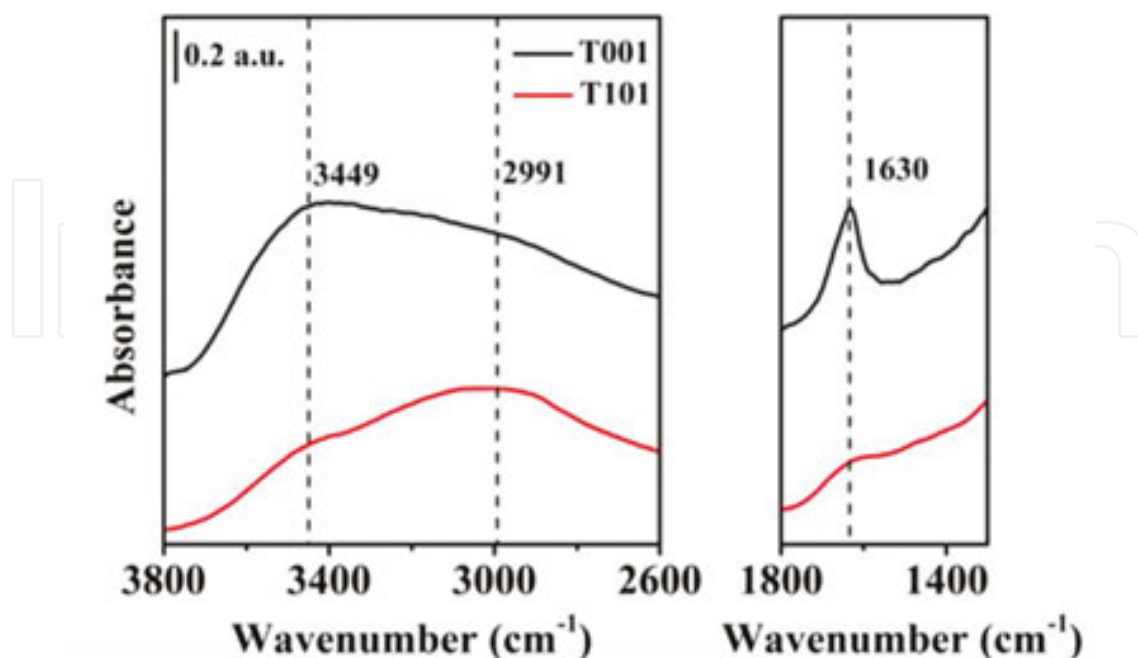
Figure 14. DRIFTS spectra of pure T001 and T101 (©2015 American Chemical Society [41]).

Wang et al. [41] identified the facet-dependent adsorption of toluene on TiO$_2$ by using an in situ DRIFTS apparatus. **Figure 14** shows the DRIFTS spectra of TiO$_2$ with dominant {001} facets (T001) and TiO$_2$ with dominant {001} facets (T101) before toluene adsorption. The bands at 3449, 2991, and 1630 cm^{-1} were assigned to O–H stretching mode of the terminal Ti–OH, adsorbed water Ti–OH$_2$ species, and H–O–H bending mode of free molecularly adsorbed water, respectively. The intensities of these bands suggested that the hydroxyl groups tend to be formed as terminal Ti–OH on the {001} facets and the {101} facets favor the formation of adsorbed water Ti–OH$_2$ species. Additionally, there is a large amount of free water on the {001} facets. **Figure 15** shows the in situ DRIFTS spectra of toluene adsorbed on T001 and T101. After toluene was introduced, the characteristic bands of toluene appeared. The positions of these bands on T101 were red-shifted slightly, compared to that on T001, which may be attributed to the different Ti^{4+} adsorption sites on {001} and {101} facets for toluene adsorption. The toluene adsorption increased more rapidly on {001} facets and the adsorption process was typically in accordance with Langmuir−Hinshelwood model of first-order reaction, while the adsorption process on {101} facets was in accordance with the two-step kinetic equation. The distinction of the adsorption capability was probably due to the different number of unsaturated 5c-Ti, capable of forming the main active adsorption sites (terminal Ti−OH species). During the photocatalytic degradation of toluene, TiO$_2$ with dominant {001} facets showed a significantly high photocatalytic activity. This outstanding performance was mainly attributed to the high adsorption ability and the preservation of the free molecularly adsorbed water, which can be dissociated to form hydroxyls and further promote the degradation.

Figure 15. In situ DRIFTS spectra of toluene adsorption on (a) T001 and (b) T101 (©2015 American Chemical Society [41]).

3.2. Degradation of formaldehyde

The adsorption and photocatalytic oxidation of formaldehyde have been frequently studied on TiO_2 with metal co-catalyst. The related mechanisms have also been investigated by in situ IR. In these cases, it was noteworthy that the formate species did not appear on pure TiO_2 without UV irradiation, indicating that the noble metal addition promoted the formation of formate species [42,43]. However, a few literature paid attention to the photocatalytic degradation process of formaldehyde on TiO_2. In the adsorption process, the interaction between

formaldehyde and the hydroxyl groups depends on hydrogen bonding. As shown in **Figure 16** [44], when water vapor was introduced, a large part of weakly adsorbed water can be detected from the broad band in the 3600–3050 cm^{-1} range and the band at 1652 cm^{-1}. However, no obvious difference about formaldehyde adsorption appears, because even in the dry condition, TiO_2 can provide the hydroxyl sites from dissociative chemisorption of water onto the Ti^{4+} sites.
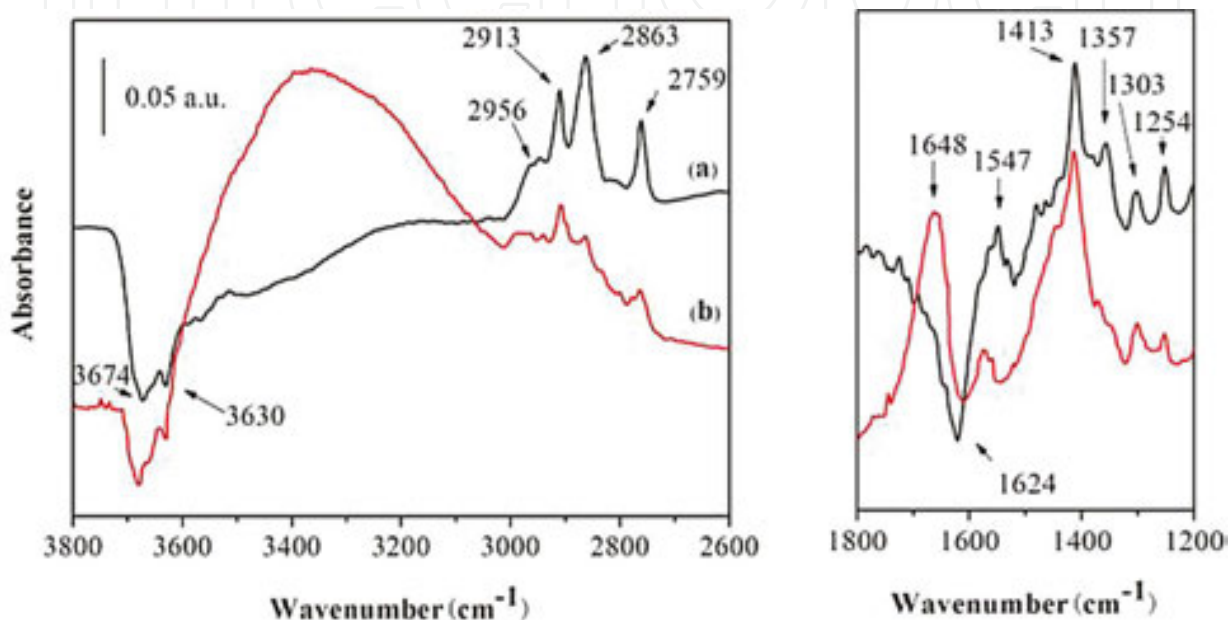
Figure 16. Differential spectra of TiO_2 after 30 min adsorption in (a) dry and (b) humidity condition (©2010 Springer [44]).

It yields significant difference after introduction of UV irradiation (**Figure 17**). In the dry condition, the bands at 2956, 2913, 2759 cm^{-1} decreased, and almost disappeared after UV irradiation for 30 min, while the bands at 2863 cm^{-1} decreased slowly relatively. All of these bands can be assigned to the C–H stretching mode υ(C–H) of formaldehyde. The small bands at low frequency (1551, 1413, 1357, 1303, and 1254 cm^{-1}) were also decreased. Meanwhile, two strong bands at 1572 and 1361 cm^{-1} appeared and reached a steady level after 30 min. The two bands could be assigned to asymmetric and symmetric υ(COO) on TiO_2 sites, respectively. These spectra suggest that the adsorbed formaldehyde converts to formate species on TiO_2. In the humidity condition, according to the changes of the integrated areas of the bands as a function of time for TiO_2 under UV irradiation, the characteristic bands of formaldehyde decrease more quickly along with quick increasing of formate species. In other words, the introduction of water promotes the conversion of adsorbed formaldehyde to formate species. It can be attributed to the fact that oxidation of water and hydroxyl groups by the photogenerated holes produces very active OH• radicals that take part in the redox reactions and improve significantly the mineralization rate of formaldehyde.
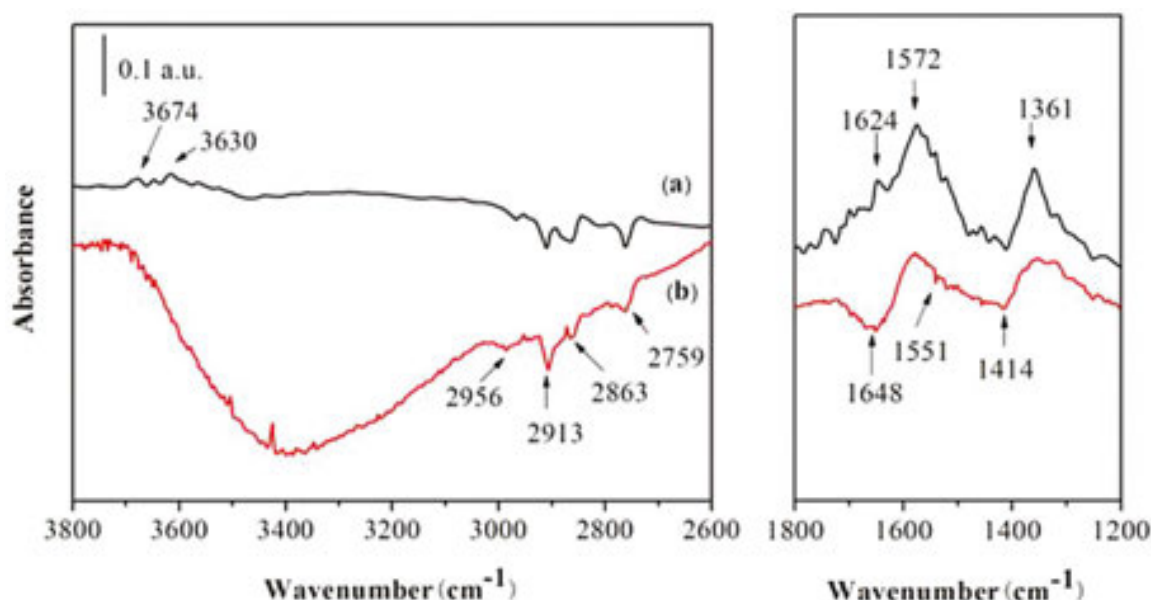
Figure 17. Differential spectra of TiO$_2$ without UV irradiation to the spectra under 30 min UV irradiation for (a) dry and (b) humidity condition (©2010 Springer [44]).

It should be pointed out that water produced during the photocatalytic process can redistribute on the surface in the form of different hydroxyl groups and further contribute to the degradation of formaldehyde. But, excessively high concentration of water vapor negatively affects the degradation efficiency because of the competitive adsorption between water and formaldehyde [46–48].

3.3. Degradation of other VOCs

The adsorption and photocatalytic oxidation of ethanol and acetone vapor on TiO$_2$ have been studied by Coronado et al. [49] using in situ DRIFTS. The in situ DRIFTS spectra obtained during the photocatalytic oxidation of ethanol and acetone vapor over TiO$_2$ powder are shown in **Figures 18** and **19**, respectively.

They found that ethanol was adsorbed on the TiO$_2$ surface either molecularly or in the form of ethoxide complexes. Acetates (the bands at 1540 and 1440 cm^{-1} can be assigned to the asymmetric and symmetric υ(COO), respectively, of acetate complexes) and formates (the band at 1360 cm^{-1} can be attributed to the symmetric υ(COO) mode of formate species) were intermediates during the photocatalytic oxidation of ethanol. In the case of acetone, it was suggested to be adsorbed exclusively in a molecular form on TiO$_2$. Acetates and formates were detected as the major intermediates and secondary intermediates, respectively. Adsorbed acetaldehyde (the peak at 1715 cm^{-1} can be assigned to the υ(C=O) vibration mode of aldehyde, and the band at 2870 cm^{-1} is characteristic of the υ(C–H) vibration of aldehyde molecules) and formic acid (the shoulder at 1745 cm^{-1} can be ascribed to the dimeric form of formic acid) were also observed. They suggested that the hydroxyl groups on the TiO$_2$ surface play a key role in the photocatalytic degradation of ethanol and acetone. However, Mattsson et al. [50] found

that the bidentate bridged formate and carbonate were the main intermediates during the photocatalytic degradation of acetone on TiO$_2$.
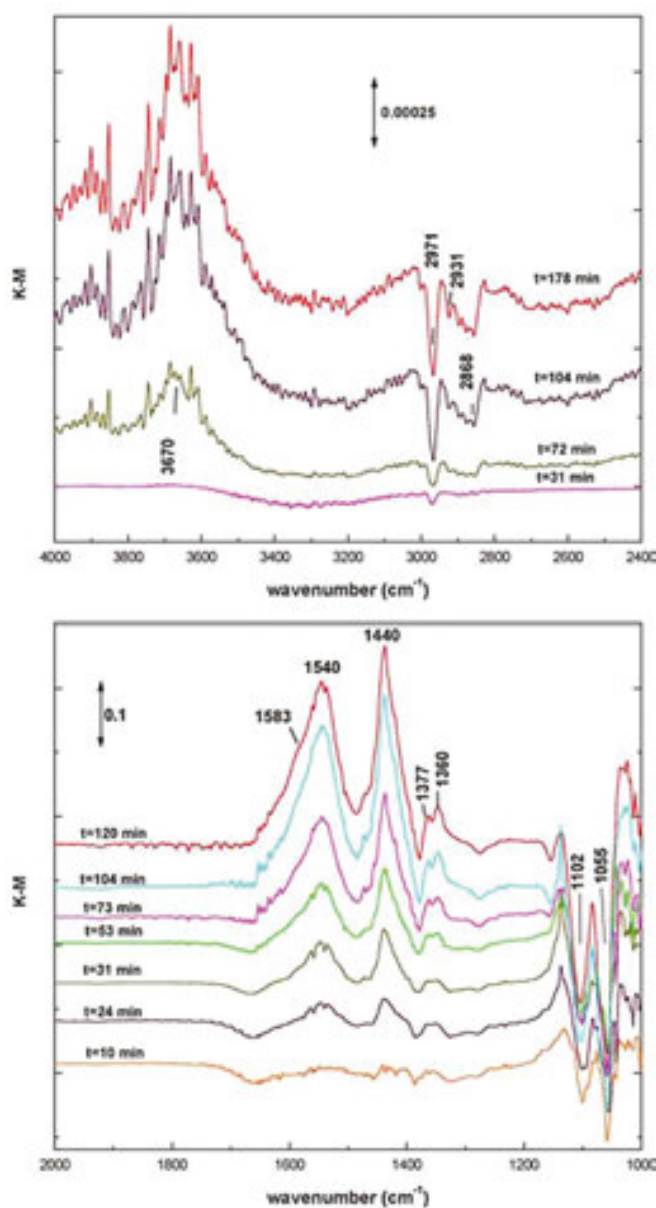
Figure 18. In situ DRIFTS spectra obtained during the photocatalytic oxidation of ethanol vapor over TiO$_2$ powder (© 2003 Elsevier [49]).

The illuminated TiO$_2$ surfaces, in the presence of methanol, were studied using in situ DRIFTS by Balcerski [51]. It was found that the irradiation of TiO$_2$ in the presence of methanol and O$_2$ produced H$_2$O, CO$_2$, and surface-bound formic acid.

An in situ DRIFTS study of acetic acid adsorption and photocatalytic oxidation on TiO$_2$ by Backes et al. [52] suggested that acetic acid adsorbed both molecularly and dissociatively as acetate on TiO$_2$. Molecularly adsorbed acetic acid was oxidized by first generation acetate.

During the photocatalytic oxidation of acetic acid on TiO_2, the α-carbon in acetate directly formed CO_2, whereas the β-carbon formed CO_2 through intermediates, such as methoxy, formaldehyde, and formate.
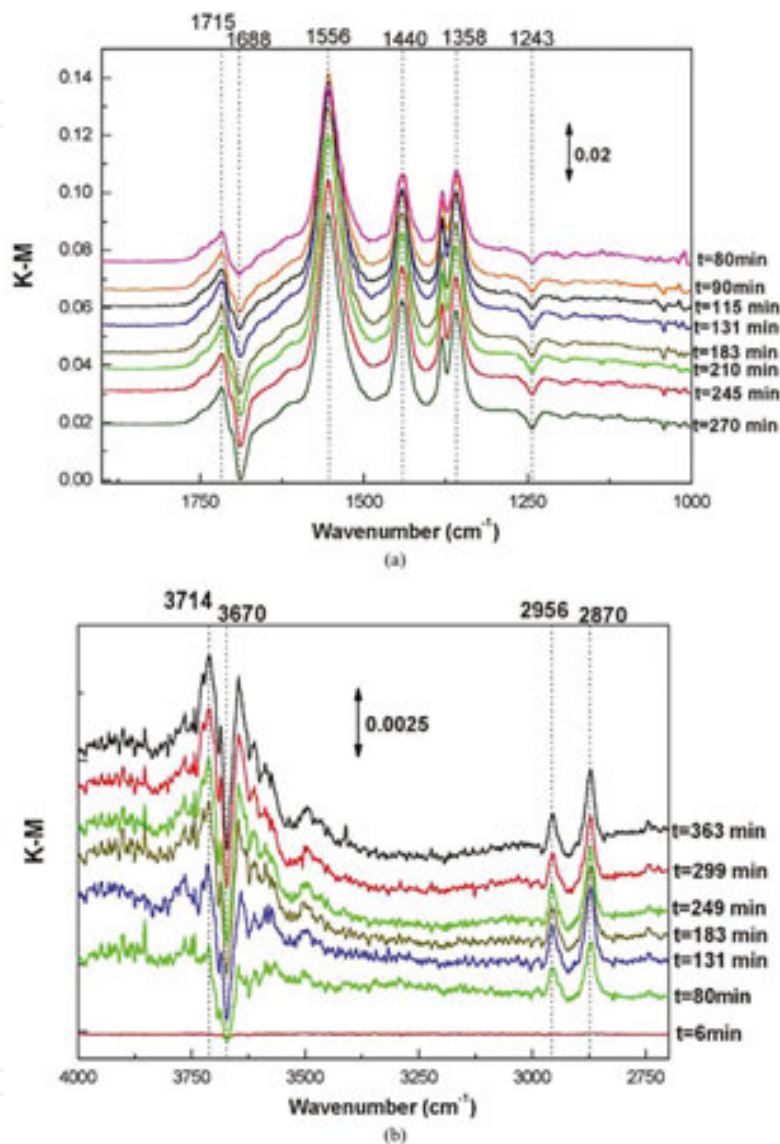

Figure 19. In situ DRIFTS spectra obtained during the photocatalytic oxidation of acetone vapor over TiO_2 powder (© 2003 Elsevier [49]).

A comparative study of the photocatalytic degradation of trichloroethylene on titanate and TiO_2 nanostructures was reported by Hernández-Alonso et al. [53]. In this study, in situ DRIFTS approach was adopted for surface analysis. They found that at least three different carboxylate species with different kinds of coordination symmetry (e.g., bridged dichloroacetate, bidentate formate, etc.) were present on the surface of the samples. The main difference between TiO_2 and nanotubes was suggested to be the larger proportion of formate species for the nanotubes. Moreover, the nanotube samples showed selective removal of some specific hydroxyl groups,

which may be due to the accumulation of carboxylate complexes (mainly dichloroacetate and formate) and/or chloride on the surface.

4. Summary and outlook

It has been demonstrated that VOCs can be efficiently photocatalytic-mineralized on TiO_2. This chapter reviewed a series of studies investigating the mechanism of photocatalytic degradation of VOCs on TiO_2 by using in situ DRIFTS. It involves in situ infrared techniques with the development of reaction cells, in situ accessories and gas-dosing systems, representative examples of spectral analyses, and special understanding of the adsorption and degradation processes. The nature of toluene, formaldehyde, and acetone, adsorbed and decomposed on TiO_2, has been obtained from in situ DRIFTS under simulated operating photocatalytic conditions. In general, surface hydroxyl groups are considered to be the major active species that the adsorption is taking place. Photogenerated charge carriers most likely react with these species to generate extremely powerful radicals which can further react with surface-adsorbed molecules of VOCs. Therefore, it drives the rising of some surface modification strategies, such as NH_3/H_2S treatment and facet engineering, to promote the performance of TiO_2. Considering that other factors, such as the oxygen adsorption, operating temperature, the initial concentration of VOCs, etc. also influence the adsorption and degradation, much work is needed to perform experiments in such conditions.

Although in situ DRIFTS is very useful to investigate the photocatalytic air purification, it should be recognized that the development of reaction cells and accessories lags behind the experimental demands. We noticed that exploiting the related accessories and gas-dosing systems is only facing limited consumer groups; therefore, it may be worthwhile expanding the success from the independent scientific group. Furthermore, coupling in situ DRIFTS with other characterization techniques, for example, gas chromatography and mass spectroscopy, is essential to obtain more kinetic information. It can be expected that further insights of in situ DRIFTS in photocatalytic air purification will be fruitful with huge amount of effort on the extension of the concept and development of instruments.

Author details

Song Sun[1*] and Fan Zhang[2]

*Address all correspondence to: suns@ustc.edu.cn

1 National Synchrotron Radiation Laboratory & Collaborative Innovation Center of Chemistry for Energy Materials, University of Science and Technology of China, Hefei, Anhui, China

2 Hefei Normal University, Hefei, Anhui, China

References

[1]   Vilcekova S, Meciarova L, International Multidisciplinary Scientific Geoconference Surveying Geology and Mining Ecology Management. 2015;1:945–952.

[2]   Sarigiannis DA, Karakitsios SP, Gotti A, Liakos IL, Katsoyiannis A, Environment International. 2011;37:743–765.

[3]   Guo H, Lee SC, Chan LY, Li WM, Environmental Research. 2004;94:57–66.

[4]   Wang S, Ang HM, Tade MO, Environment International. 2007;33:694–705.

[5]   Lin L, Chai Y, Zhao B, Wei W, He D, He B, Tang Q, Open Journal of Inorganic Chemistry. 2013;3:14–25.

[6]   Fujishima A, Rao TN, Tryk DA, Journal of Photochemistry and Photobiology C: Photochemistry Reviews. 2000;1:1–21.

[7]   Dhada I, Nagar PK, Sharma M, Industrial & Engineering Chemistry Research. 2015;54:5381–5387.

[8]   Chen H, Nanayakkara CE, Grassian VH, Chemical Reviews. 2012;112:5919–5948.

[9]   Pelaez M, Nolan NT, Pillai SC, Seery MK, Falaras P, Kontos AG, Dunlop PSM, Hamilton JWJ, Byrne JA, O'Shea K, Entezari MH, Dionysioua DD, Applied Catalysis B: Environmental. 2012;125:331–349.

[10]   Ryczkowski J, Catalysis Today. 2001;68:263–381.

[11]   Lukaski AC, Muggli DS, Journal of Catalysis. 2004;223:250–261.

[12]   Pichat P, Catalysis Today. 2014;224:251–257.

[13]   Dolamic I, Bürgi T, Journal of Catalysis. 2007;248:268–276.

[14]   Hunger M, Weitkamp J, Angewandte Chemie International Edition. 2001;40:2954–2971.

[15]   Cao L, Gao Z, Suib SL, Obee TN, Hay SO, Freihaut JD, Journal of Catalysis. 2000;196:253–261.

[16]   Griffiths PR, de Haseth JA, Fourier Transform Infrared Spectroscopy. 2nd ed. A John Wiley & Sony Inc. Publication; 2007.

[17]   Zhang F, Wang M, Zhu X, Hong B, Wang W, Qi Z, Xie W, Ding J, Bao J, Sun S, Gao C, Applied Catalysis B: Environmental. 2015;170:215–224.

[18]   Zhang F, Zhu X, Ding J, Qi Z, Wang M, Sun S, Bao J, Gao Ch, Catalysis Letters. 2014;144:995–1000.

[19]   Deveau PA, Arsac F, Thivel PX, Ferronato C, Fe Delpech, Chovelon JM, Kaluzny P, CMonnet, Journal of Hazardous Materials. 2007;144:692–697.

[20]   Kozlov DV, Paukshtis EA, Savinov EN, Applied Catalysis B: Environmental. 2000;24:L7–L12.

[21]   Zheng C, Li X, Zhao Q, Qu Z, Quan X, Separation and Purification Technology. 2009;67:326–330.

[22]   Hauchecorne B, Tytgat T, Terrens D, Vanpachtenbeke F, Lenaerts S, Infrared Physics & Technology. 2010;53:469–473.

[23]   Xu J, Chen Q, Ji H, Progress in Chemistry. 2008;20:811–820.

[24]   Wood J, Alldrick MJ, Winterbottom JM, Stitt EH, Bailey S, Catalysis Today. 2007;128:52–62.

[25]   Zhang M, Zhang W, Xie W, Qi Z, Wu G, Lv M, Sun S, Bao J, Journal of Molecular Catalysis A: Chemical. 2014;395:269–275.

[26]   Turchi CS, Ollis DF, Journal of Catalysis. 1990;122:178–192.

[27]   Henderson MA, Surface Science Reports. 2011;66:185–297.

[28]   Andreozzi R, Caprio V, Insola A, Marotta R, Catalysis Today. 1999;53:51–59.

[29]   Quici N, Vera ML, Choi H, Puma GL, Dionysiou DD, Litter MI, Destaillats H, Applied Catalysis B: Environmental. 2010;95:312–319.

[30]   Lee SL, Scott J, Chiang K, Amal R, Journal of Nanoparticle Research. 2009;11:209–219.

[31]   Davit P, Martra G, Coluccia S, Journal of the Japan Petroleum Institute. 2004;47:359–376.

[32]   Farfan-Arribas E, Madix RJ, Journal of Physical Chemistry B. 2003;107:3225–3233.

[33]   Hadjiivanov KI, Klissurski DG, Chemical Society Reviews. 1996;25:61–69.

[34]   Augugliaro V, Coluccia S, Loddo V, Marchese L, Martra G, Palmisano L, Schiavello M, Applied Catalysis B: Environmental. 1999;20:15–27.

[35]   Maira AJ, Coronado JM, Augugliaro V, Yeung KL, Conesa JC, Soria J, Journal of Catalysis. 2001;202:413–420.

[36]   Ibusuki T, Takeuchi K, Atmospheric Environment. 1986;20:1711–1715.

[37]   Zhao J, Yang XD, Building and Environment. 2003;38:645–654.

[38]   Li X, Zou X, Qu Z, Zhao Q, Wang L, Chemosphere. 2011;83:674–679.

[39]   Méndez-Román R, Cardona-Martínez N, Catalysis Today. 1998;40:353–365.

[40]   Sun S, Ding J, Bao J, Gao C, Qi Z, Yang X, He B, Li C, Applied Surface Science. 2012;258:5031–5037.

[41]   Wang M, Zhang F, Zhu X, Qi Z, Hong B, Ding J, Bao J, Sun S, Gao C, Langmuir. 2015;31:1730–1736.

[42] Zhang C, He H, Tanaka K, Applied Catalysis B: Environmental. 2006;65:37–43.

[43] RaskóJ, Kecskés T, Kiss J, Journal of Catalysis. 2004;224:261–268.

[44] Sun S, Ding J, Bao J, Gao C, Qi Z, Li C, Catalysis Letters. 2010;137:239–246.

[45] Obee TN, Brown RT, Environmental Science and Technology. 1995;29:1223–1231.

[46] Martra G, Coluccia S, Marchese L, Augugliaro V, Loddo V, Palmisano L, Schiavello M, Catalysis Today. 1999;53:695–702.

[47] Ao CH, Lee SC, Yu JZ, Xu JH, Applied Catalysis B: Environmental. 2004;54:41–50.

[48] Yang J, Li D, Zhang Z, Li Q, Wang H, Journal of Photochemistry and Photobiology A: Chemistry. 2000;137:197–202.

[49] Coronado JM, Kataoka S, Tejedor-Tejedor I, Anderson MA, Journal of Catalysis. 2003;219:219–230.

[50] Mattsson A, Leideborg M, Larsson K, Westin G, Österlund L, Journal of Physical Chemistry B. 2006;110:1210–1220.

[51] Balcerski W, SY Ryu, MR Hoffmann, International Journal of Photoenergy. 2008;2008:964721.

[52] Backes MJ, Lukaski AC, Muggli DS, Applied Catalysis B: Environmental. 2005;61:21–35.

[53] Hernández-Alonso MD, García-Rodríguez S, Suárez S, Portela R, Sánchez B, Coronado JM, Catalysis Today. 2013;206:32–39.